

# A Numerical Model of Manganese Distribution in Pancreatic Tissue from meMRI measurements

Ekkehard Küstermann<sup>1</sup>, Anke Meyer<sup>2</sup>, Katharina Stolz<sup>2</sup>, Wolfgang Dreher<sup>1</sup>, and Kathrin Maedler<sup>2</sup>

<sup>1</sup>AG "in-vivo-MR", FB2, Universität Bremen, Bremen, Germany, <sup>2</sup>Center for Biomolecular Interactions Bremen, Universität Bremen, Bremen, Germany

**Introduction:** Diabetes research and therapy will benefit from non-invasive methods of analyzing pancreatic beta-cell mass (BCM) and function. A promising strategy is the measurement of paramagnetic manganese ( $Mn^{2+}$ ) uptake in pancreatic tissue by  $T_1$ -weighted *in-vivo* MR imaging (meMRI) [1-8]. Due to the similarity of their physical properties to calcium ions ( $Ca^{2+}$ ),  $Mn^{2+}$  ions enter metabolically active  $\beta$ -cells through voltage-gated calcium channels, which open in response to a rise in extracellular glucose [9,10]. The time course of the  $T_1$ -weighted MR-signal upon a bolus injection of  $Mn^{2+}$  allows the extraction of detailed information about the metabolic processes in the tissue of interest. These observed signal changes were appropriately mathematically modeled based on exponential functions [1-3] while washout-processes were characterized by a linear function [3]. Careful inspection of *in vivo* MRI data from diabetic and non-diabetic mice revealed a considerable variability between exponential and sinusoidal characteristics combined with linear bias. Time courses of individual experiments from liver, pancreas and kidney shared similar temporal features, which suggest that the availability of manganese ions varies individually despite the reproducible initial bolus injection. The rate of signal change was always the fastest in the liver and reaches a plateau after about 30 min. The liver signal was used as input control reflecting the availability of  $Mn^{2+}$ . In order to account for individual variability, the signal time course of pancreatic tissue was analyzed with a mathematical model consisting of three sequentially ordered compartments: a source ("0") and two pancreatic compartments ("1" and "2"). The metabolism was characterized by estimating both fluxes between the compartments and the fractional volume sizes of pancreatic tissue.

**Methods:** *MRI:* All measurements were performed at 7T MR Scanner (Bruker BioSpec 70/20) with a quadrature volume coil for RF transmission and reception. 3D-"Snapshot FLASH" images with inversion recovery preparation were acquired for kinetic measurements of the  $Mn^{2+}$  uptake [11]. One image without inversion served as the referential  $^1H$ -density measurement. The 3D encoding scheme permits the spin inversion over the entire body and thus reduces the sensitivity against inevitable body motion between inversion pulse and signal readout. The  $TI=700ms$  was a compromise between sensitivity for  $Mn^{2+}$ -uptake and preservation of residual signal for tissue discrimination. A TR of 6s ensured full relaxation and avoided breathing rate dependent  $T_1$ -effects. Mice received glucose (2g/kg i.p.) maximum 30min before  $MnCl_2$  (8mg/kg i.v.) and were anesthetized by isoflurane. *Metabolic Model:* The 3-compartment model (Fig. A) was encoded in Matlab by a system of coupled differential equations, which were solved by an ODE solver and fitted in a least-square sense (Levenberg-Marquardt algorithm) to the experimental signal time course data from pancreatic tissue. The maximal signal intensity is taken from the reference scan. Fluxes describe the label flow per time and follow the concentration differences between compartments. Fluxes and the volume ratio of compartments "1" and "2" are estimated to give the best fit of the acquired MR data (Fig. B).

**Results:** The metabolic model allows exact fitting of the acquired data in diabetic as well as non-diabetic mice, the fit catches almost all measured data (see Fig. B). From repetitive measurements ( $n=10$ ) of a mouse over 17 weeks the input-flux  $F_1$  is estimated to be so large that the  $Mn^{2+}$ -concentration in the first pancreatic compartment behaves exactly as in the liver (flux constant:  $f_1 = 4.3 \pm 3.7 s^{-1}$ ). The size of this first compartment is estimated as about half of the second compartment ( $V_1/V_2 = 0.35/0.65 \pm 0.09$ ), which is supplied with manganese much slower (flux constant  $f_2 = 7.2 \cdot 10^{-4} \pm 4.0 \cdot 10^{-4} s^{-1}$ ) and contributes almost linearly to the temporal development of the MR-signal. Interestingly, if no glucose is given ( $n=1$ ), the observed signal can be explained by  $Mn$ -accumulation in compartment "1" only (Fig.B left), while the second compartment always is filled after glucose application (Fig.B right).

**Discussion and Conclusions:** We are aware that the resolution of dynamic *in-vivo* MR imaging is barely suited to detect individual islets [5]. Especially under the constraints of our fast,  $T_1$ -sensitive and motion-insensitive MR imaging, the  $\beta$ -cell tissue of interest may comprise only a partial volume of an image voxel [11]. Nevertheless, this metabolic model allows to dissect the measured MR-signal of pancreatic tissue unambiguously in two components of very different temporal characteristics: (i) a small compartment with nearly the same temporal development as the liver (expressed in the model by an almost instantaneous exchange with the  $Mn^{2+}$ -delivering source) and (ii) a larger compartment characterized by a much slower change of signal and  $Mn^{2+}$  concentration. This second component reflects the metabolic activity of interest while the first is likely to represent any passive uptake of  $Mn^{2+}$ -ions by the pancreatic tissue. The signal time course of the first component is nearly identical to that of the liver but was still modeled in order to be able to identify temporal changes in treated animals. This analysis and modeling of time course data is key to the interpretation of meMRI data and the understanding of pathophysiological processes during diabetes progression.

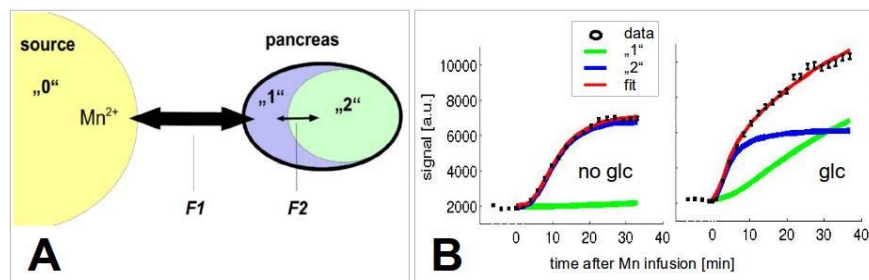


**Fig. A:** Metabolic Model: F describes the flux between compartments. The areas and the thickness of arrows reflect the estimated results.

**Fig. B:** Representative fit of the model to individual experiments (black). Data represent the mean signal of pancreas after  $MnCl_2$  injection.

Error bars=SEM. **Left:** without glucose stimulation. **Right:** after glucose stimulation.

**References:** [1] Antkowiak, P.F. et al. *Am J Physiol Endocrinol Metab* 296:E573 (2009)

[2] Antkowiak, P.F. et al. *MRM* 67:1730 (2012)

[4] Gimi, B. et al. *Cell Transplant* 15:195 (2006)

[6] Leoni, L. et al. *Contrast Media Mol Imag* 6:474 (2011)

[8] Nagata, M. et al. (2011) *Radiol Phys Technol* 4:7

[10] Dyachok, O. et al. *J Cell Sci* 114: 2179 (2001)

[3] Dhyani, A.H. et al. *MRI* 31:508 (2013)

[5] Lamprianou, S. et al. *Diabetes* 60:2853 (2011)

[7] Leoni, L. et al. *Curr Pharm Des* 16:1582 (2010)

[9] Ashcroft, F.M. et al. *Prog Biophys Mol Biol* 54:87 (1989)

[11] Küstermann, E. et al. *Proc. Intl. Soc. Mag. Reson. Med.* 19:810 (2011)